

GC Quantifying Shallow Seismic Anomalies*

Ritesh Kumar Sharma¹ and Satinder Chopra¹

Search and Discovery Article #42101 (2017)

Posted June 26, 2017

*Adapted from the Geophysical Corner column, prepared by the authors, in AAPG Explorer, June, 2017. Editor of Geophysical Corner is Satinder Chopra (schopra@arcis.com). Managing Editor of AAPG Explorer is Brian Ervin. AAPG © 2017

¹Arcis Seismic Solutions, TGS, Calgary, Canada (schopra@arcis.com)

General Statement

The determination of properties such as lithology, fluid content, porosity and permeability help us characterize a subsurface reservoir. Such an exercise can be taken to the next step with the determination of petrophysical properties such as water saturation and volume of clay, which can aid the appraisal of a reservoir. All these properties can be obtained by lab measurements on core samples, or by carrying out petrophysical analysis on log curves, which are only possible at well locations. But as is generally the case, our goals are to characterize reservoirs not vertically, but spatially, and thus we turn to seismic data for their determination.

Impedance Inversion

The usual workflows for seismic differentiation between lithology and fluid content take advantage of their relationships between different elastic constants such as bulk modulus (measure of incompressibility of the rock), shear modulus (measure of rigidity) and Young's modulus (measure of stiffness), which can be seismically derived through the process of impedance inversion. Impedance inversion transforms seismic amplitudes, both prestack and poststack, into impedance values. There are different methods of impedance inversion, which we have described in our series of Geophysical Corner articles:

[Impedance Inversion Transforms Aid Interpretation, Search and Discovery article #41622](#)

[Prestack Impedance Inversion Aids Interpretation, Search and Discovery article #41664](#)

[Joint Impedance Inversion Transforms Aid Interpretation, Search and Discovery article #41667](#)

In prestack seismic data, as the fluid/lithology information resides on the far offsets, or large angles of incidence, a promising approach is the analysis of impedance with respect to different offsets/angles. Such a workflow is referred to as elastic impedance, which we described with examples in our article [An 'Elastic Impedance' Approach, Search and Discovery article #41082](#).

But when it comes to the determination of petrophysical properties such as water saturation, effective porosity and permeability, an extension of the elastic impedance approach, called “extended elastic impedance” is utilized. The basic idea behind this workflow is that though typically the incident angle range is 0 to 30 degrees, it can be mathematically extended to a greater angle range, and by modifying the Zoeppritz formulation, extended elastic impedance reflectivities at different angles can be generated. By cross-correlating these generated reflectivities with the desired petrophysical property, the optimum angle can be determined, which can then be used to derive the desired petrophysical property from seismic data.

Accounting for High Amplitude Anomalies

In [Characterizing Shallow Seismic Anomalies, Search and Discovery article #42086](#) we described the characterization of shallow high amplitude seismic anomalies in the Hoop Fault Complex area of Barents Sea that hosts shallow and deep-seated hydrocarbon accumulations. In particular, the objectives were to explore for potential reservoir prospects within the Mid-Jurassic StØ and Mid-Triassic Kobbe formations, encompassing the Snadd Formation in-between.

As we mentioned in that article, there could be various reasons for high amplitude anomalies to show up on seismic data, and it is our objective to distinguish those seismic anomalies that are associated with hydrocarbons from those that are not. We demonstrated the application of spectral decomposition as direct hydrocarbon indicator that qualitatively identifies the hydrocarbon bearing zones. We pursue that exercise further with the application of extended elastic impedance approach. In [Figure 1a](#) we show the workflow followed in this exercise. As we cross-correlate the extended elastic impedance reflectivities with the desirable V_{clay} and effective porosity log curves for different values of the angles, we plot the correlation coefficients as shown in [Figure 1b](#). The maximum positive correlation coefficient of 0.85 for V_{clay} (green curve) is seen at 28 degrees, while effective porosity exhibits a negative correlation coefficient of 0.9 at angle 22 degrees (blue curve). These values of angle enable the determination of these properties from seismic data through the application of Zoeppritz equations.

In [Figure 2](#) we exhibit equivalent cross-line sections from the effective porosity and V_{clay} volumes with the respective petrophysical log curves overlaid on them. A reasonably good match between them is seen in both cases, which enhances our confidence in the application of the followed approach for the data at hand.

We take this analysis further and crossplot effective porosity and V_{clay} derived attributes as shown in [Figure 3a](#). Next, we enclose the cluster of points that exhibit high porosity and low values, or not-so-high values of V_{clay} with red, green and blue polygons, and backproject them on the vertical seismic. The latter step helps us understand where these cluster of points are coming from in the different zones of interest. In [Figure 3b](#) we see the differentiation of the potential reservoirs within the three formations of interest, namely the StØ, Snadd and Kobbe formations.

Conclusion

In conclusion, we have characterized the direct hydrocarbon anomalies that we detected through the application of spectral decomposition, with more detailed analysis employing extended elastic impedance for deriving effective porosity and volume of clay from seismic data. The good correlation of these volumes with the available respective petrophysical well log curves has enhanced our confidence in their interpretation.

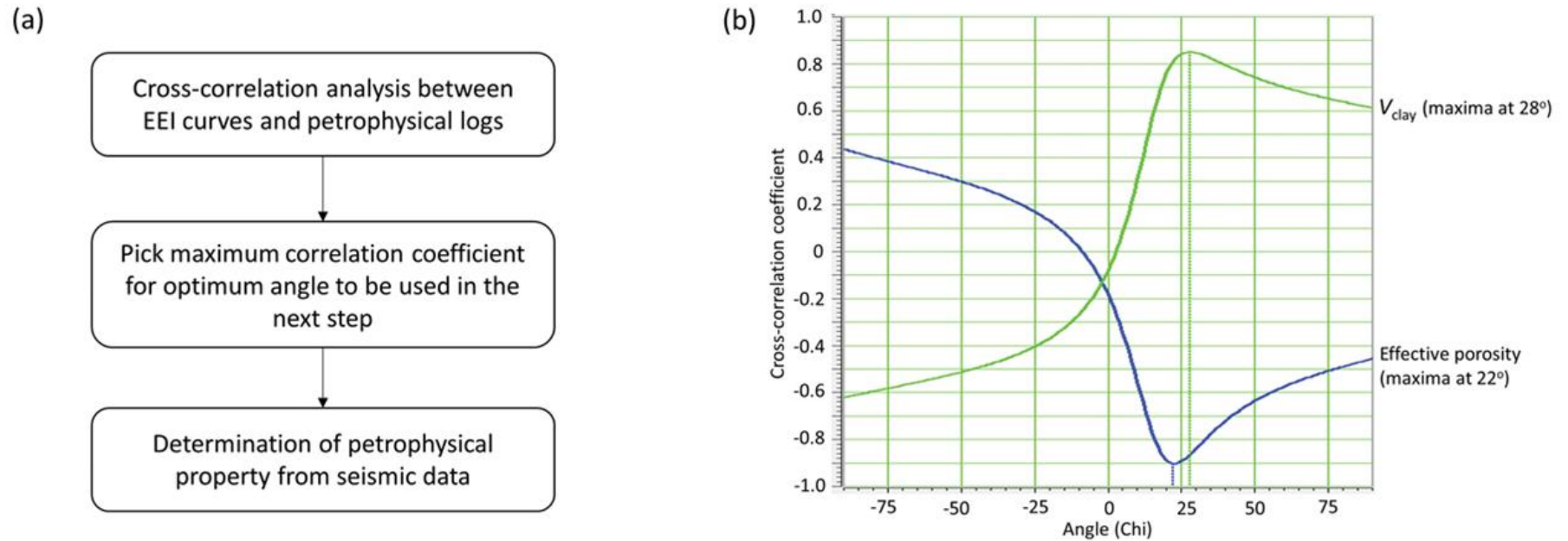


Figure 1. (a) Workflow for extended elastic impedance (EEI) approach for predicting the volume of petrophysical properties from seismic data. (b) Cross-correlation analysis for effective porosity (blue curve) and V_{clay} (green curve) with EEI curves. A maximum negative correlation is seen for effective porosity at 28 degrees, and a maximum positive correlation is seen for V_{clay} at 22 degrees.

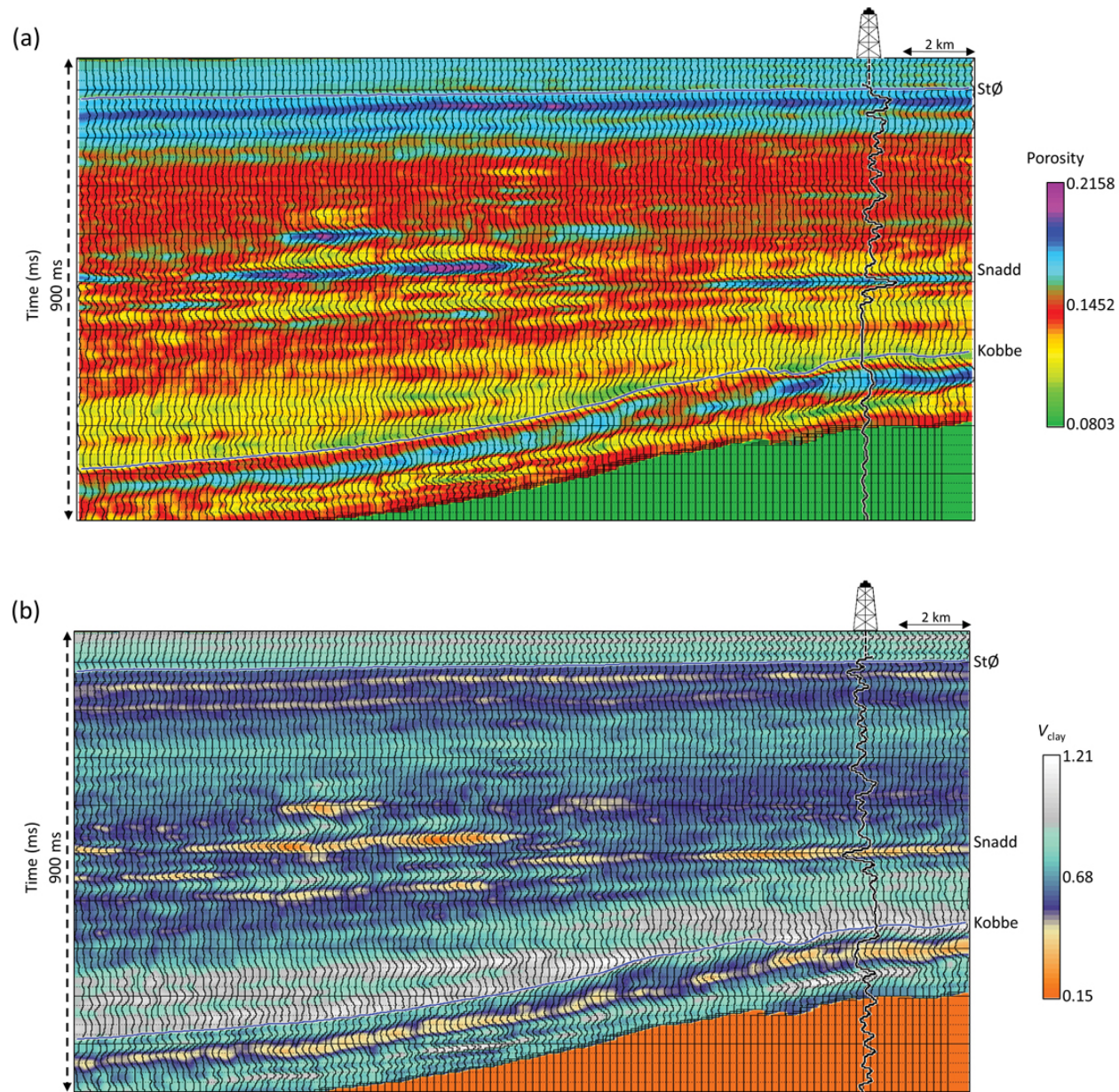


Figure 2. (a) A cross-line section from inverted effective porosity volume passing through a well. The overlaid effective porosity curve shows a strong correlation with inverted results. (b) Equivalent cross-line section from inverted V_{clay} volume passing through a well. The overlaid V_{clay} curve shows a strong correlation with inverted results. (Data courtesy: TGS, Asker, Norway)

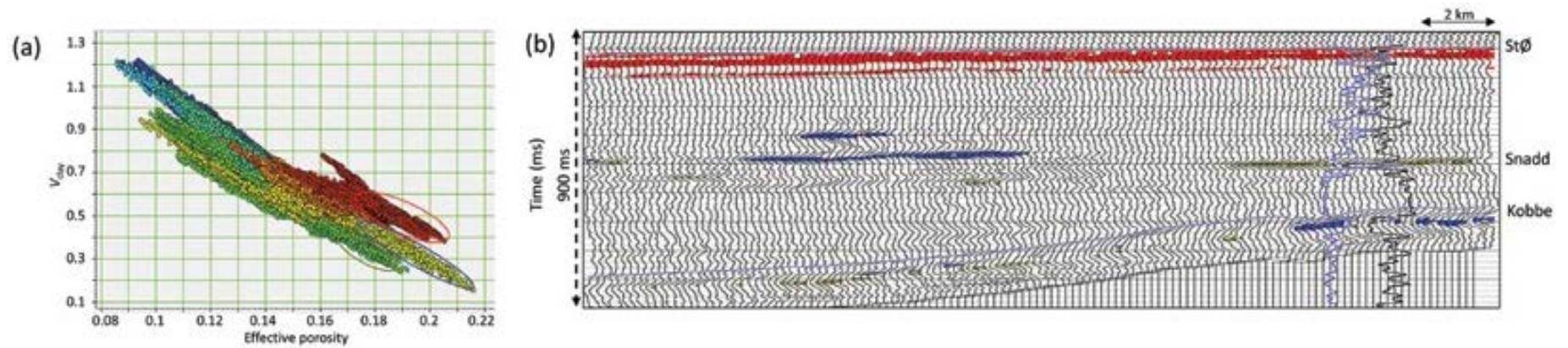


Figure 3. (a) Cross-plot of inverted effective porosity and V_{clay} volumes over the zone of interest. Cluster of points exhibiting high porosity and low V_{clay} values are enclosed by red, green and blue polygons. The back projection of these polygons on the seismic cross-line is shown in (b). Notice we are able now to differentiate the potential reservoirs within StØ, Snadd and Kobbe formations.